Coupling of Magnetic and Fluid Flow Problems and its Application in Induction Melting Apparatus

by G. Henneberger, Ph. K. Sattler, D. Shen, W. Hadrys
Institute of Electrical Machines,
University of Technology Aachen
Schinkelstrasse 4, 5100 Aachen, Germany

Abstract – **The paper describes the way of computation for the calculation of the magnetic and fluid flow field in induction melting apparatus. The Finite Element Method will be used for the determination of the magnetic field. On the other hand the calculation of the fluid flow field is done using the Finite Difference Method. Also of importance is the precalculation of the surface shape for which a method will be presented because it influences on the induced melting power.**

I. INTRODUCTION

Induction melting apparatus are widely used in industry for melting and alloying of metals, especially cast iron, aluminum and copper. The principle is to use the power losses from the eddy currents in the crucible for the heating of the melt. Simultaneously there will be a fluid field in the melt as a result of the electromagnetic Lorentz forces. This fluid field is used for intermixing the melt but is causes also a typical surface shape the quantity of which depends upon the melting power and the frequency of the current.

A complete understanding of the magnetic field is imperative to predict and control the magnetic and electrical quantities such as the melting power, the efficiency, the currents and voltages of the melting apparatus. Also of interest are the elements of the equivalent circuit diagram.

Besides the magnetic field it is very important in metallurgy to predict and control the behaviour of the fluid flow, especially its velocity and spatial distribution as well as the form of the free surface.

II. CONSTRUCTION OF A CRUCIBLE FURNACE

Fig. 1 shows the main components of a crucible furnace. The crucible containing the melt is built up by fire-clay. The coil described here as a simple rectangle consists of 8 to 20 windings. The shape of the coil can be built up in a rectangle or a circle or as a combination of these two basic shapes. The coil is water-cooled and its efficiency is about 70% to 80% depending upon the melting material. Another main part are the yokes. 8 to 10 of them are placed around the coil at regular intervals.

III. COMPUTATION METHODS

The coupled problem consists of the solution of a magnetic and a fluid flow problem. The distinctions between these two problems are the complexity of the geometry and the characteristics of the governing equations. When dealing with the fluid flow problem only the crucible including the melt has to be examined. By way of contrast the magnetic computation has to take into consideration the crucible with the melt as the eddy current region, the yokes, the coil and the entire surrounding air region. A very different discretisation density of the chosen mesh is necessary in the analysis region. On the one hand the surrounding air region can be considered with a coarse mesh but on the other hand the eddy current region in the crucible has to be subdivided with a fine mesh. The finite element method with its flexible subdivisions is most suitable for this application. The discretisation density of the field of flow can be chosen as a homogeneous one because of the simple geometry in the crucible. This is one reason for using the finite element method in the numerical processing of the Navier-Stokes equation.

On the other side both fields are very closely coupled. The linkage is the Lorentz-force in the eddy current region. The magnetic field determines the distribution of the force density and simultaneously the movement of the melt. The movement of the melt again influences the free surface form. This alternation of the melt's geometry also changes the geometry of the eddy current region in the magnetic computation. It becomes clear that the solution of the whole problem can only be done by an iterative process.

In this contribution a method is developed to compute the coupled problem of the magnetic and fluid field. Its application to an industrial crucible furnace will be presented.

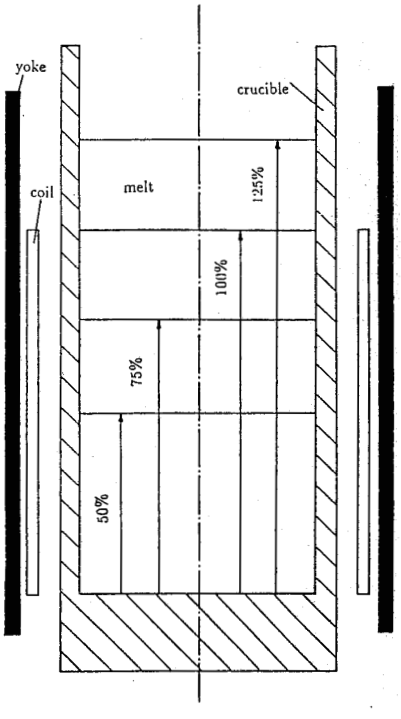

Figure 1: Crucible furnace for 2000 kg cast iron

IV. MAGNETIC FIELD

The treatment of the magnetic field consists of the solution of an axisymmetric eddy current problem using Maxwell's equations in time harmonic formulation

$$\nabla \times \vec{H} = \sigma \vec{E} + \vec{J}^e \quad (1)$$

$$\nabla \times \vec{E} = -j\omega \vec{B} \quad (2)$$

and the equations which describe the material properties

$$\vec{H} = \frac{1}{\mu}\vec{B} \quad (3)$$

$$\vec{J} = \sigma \vec{E} \quad (4)$$

where μ is the permeability, σ the conductivity and $f = \omega/2\pi$ the frequency. $\vec{H}$ is the magnetic and $\vec{E}$ the electrical field strength, $\vec{J}^e$ and $\vec{J}$ are the source and the induced current density. With the definition of the vector potential $\vec{A}$

$$\vec{B} = \nabla \times \vec{A} \quad (5)$$

the following Helmholtz equation for $\vec{A}$ can be derived from eq. (1) to (5)

$$\nabla \times \vec{A} = -j\omega\mu\sigma\vec{A} + \mu\vec{J}^e \quad (6)$$

As a consequence of the axial symmetry the vector potential $\vec{A}$ only includes the φ - component. The numerical solution of eq. (6) using the finite element method is done with reference to [1,12]. Fig. 2 shows some flux line plots at different load levels. The frequency is 316Hz , the current density in the coil is $3.57\mathrm{A/mm^2}$ in each case. The load levels are 50%, 75%, 100% and 125% relating to the length of the coil. It is of importance to notice that the leakage field becomes as larger as the load level of the melt in the crucible becomes lower. This has consequences for the circulation of the force distribution which will be described later. Fig. 3 shows the effect of the current displacement in the melt at a constant load level of 100%. The magnetic field is pushed to the direction of the crucible and remains in a small area whose penetration depth δ can be calculated by the equation

$$\delta = \frac{1}{\sqrt{\pi f \sigma \mu}} \quad (7)$$

At higher frequencies the radial component at the free surface and the bottom of the crucible becomes more and more large. This causes big circulations of force in these regions whose effects will be discussed later.

V. FIELD OF FLUID FLOW

The behaviour of the fluid is described by the equation of Navier-Stokes

$$\nabla(\frac{1}{2}\vec{v}^2) - \vec{v} \times (\nabla \times \vec{v}) = \quad (8)$$

$$= -\nabla(gz) - \frac{1}{\rho}(\nabla p - \vec{f}_{el}) + \frac{Rv_B}{Re}\Delta\vec{v}$$

$$\mathrm{Re} = \frac{v_B\, R\, \rho}{\eta} \quad (9)$$

$\vec{v}$ describes the field of velocity in the melt, g the acceleration of gravity, p the pressure function, Re is the Reynolds number being determined by (v_B) the characteristic velocity, (R) the characteristic length, (ρ) the mass density and (η) the viscosity and $\vec{f}_{el}$ characterizes the vector field of the Lorentz forces. z is the coordinate in the vertical direction. As a consequence of the axial symmetry of the crucible it is advantageous to use an axisymmetric coordinate system and to introduce the stream function $\vec{\Psi}$ and the vorticity vector $\vec{\Omega}$ because of the reduction of unknowns and the more convenient formulation of the field values on the borders.

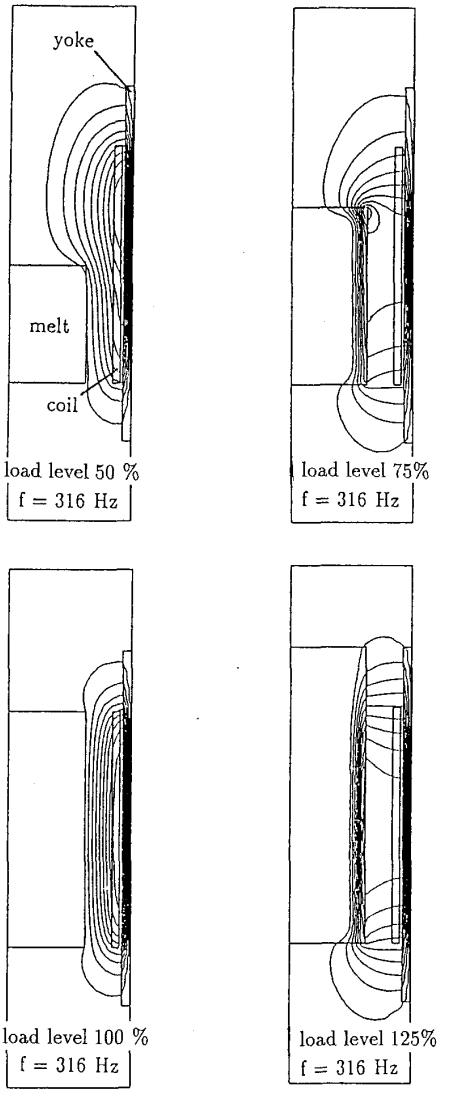

Figure 2: flux lines at different load levels – geometry relating to Fig. 1

Only the φ - component of the stream function vector $\vec{\Psi}$ is non-zero, and using the notation $\vec{\Psi} = \Psi \cdot \vec{e_\varphi}$ the following definition is valid

$$\vec{v} = \nabla \times (\frac{\Psi}{r}\vec{e}_\varphi)\,. \quad (10)$$

The defining equation (10) complies with the continuity equation

$$\nabla \cdot \vec{v} = 0 \quad (11)$$

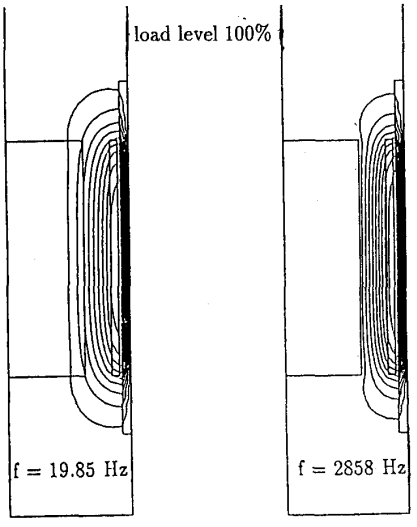

Figure 3: flux lines at different frequencies – geometry relating to Fig. 1

automatically. The vorticity vector $\vec{\Omega}$ is defined using the relation

$$\vec{\Omega} = \Omega \vec{e}_\varphi = \nabla \times \vec{v} \tag{12}$$

Performing the curl of eq. (8) and taking into consideration the eq. (10) and (12) the Navier-Stokes equation can be written as

$$0 = \nabla \times \vec{f}_{el} - \frac{\partial(u\,\Omega)}{\partial r} - \frac{\partial(w\,\Omega)}{\partial z} + \frac{1}{\mathrm{Re}}\{\frac{\partial^2 \Omega}{\partial r^2} + \frac{1}{r}\frac{\partial \Omega}{\partial r} - \frac{\Omega}{r^2} + \frac{\partial^2 \Omega}{\partial z^2}\} \tag{13}$$

$$\vec{v} = (u, 0, w) = u(r,z)\,\vec{e}_r + w(r,z)\,\vec{e}_z \tag{14}$$

$$u = -\frac{1}{r}\frac{\partial \Psi}{\partial z} \quad , \quad w = \frac{1}{r}\frac{\partial \Psi}{\partial r} \tag{15}$$

Regarding the governing equation for the stream function Ψ eq. (10) and (12) can be used to write

$$\frac{\partial^2 \Psi}{\partial r^2} - \frac{1}{r}\frac{\partial \Psi}{\partial r} + \frac{\partial^2 \Psi}{\partial z^2} = -r\,\Omega \tag{16}$$

From now on the fluid flow problem is described as a boundary value problem of two elliptic partial differential equations. For the boundary conditions the following relations can be derived

Ψ	Ω	boundary	
$\Psi_1 = 0$	0	axis of the crucible	(17)
$\Psi_2 = 0$	0	free surface	(18)
$\Psi_3 = 0$	$-\frac{1}{r}\cdot\frac{\partial^2\Psi}{\partial r^2}$	side of the crucible	(19)
$\Psi_4 = 0$	$-\frac{1}{r}\cdot\frac{\partial^2\Psi}{\partial z^2}$	bottom of the crucible	(20)

The turbulent fluid flow is taken into account by the effective viscosity η_W [2]. For the free turbulent circle vortex we have

$$\frac{\eta_W}{\eta} = \frac{\mathrm{Re}}{\mathrm{Re}_{min}} \tag{21}$$

where Re_{min} has been determined by experiment. In this case we take the value $\mathrm{Re}_{min} = 30$ [2,5]. The vortex in the metal fluid stream bath approaches the free turbulent circle whirlpool, with the exception of the crucible's side.

The free surface form of the melt is adapted to the pressure, the velocity and the electromagnetic forces by the governing equation

$$\frac{\partial p}{\partial t} = 0 \tag{22}$$

In eq. (22) $\vec{t}$ describes the unit vector in the tangential direction to the surface (Fig. 4).

The computation of the free surface form of the melt is performed using the following equation

$$\nabla p = -\nabla(\frac{\rho}{2}\vec{v}^2) + \vec{f}_{el} - \rho g \vec{e}_z \;, \tag{23}$$

which is a generalized Bernoulli equation. Taking into consideration eq. (23) the form of the free surface has to be corrected as long as the relation $\nabla p = 0$ with reference to eq. (22) is fulfilled [3]. This is also an iterative process. Because of the simple geometry of the crucible the reliable method of finite differences is used for the numerical computation. The existence of the term

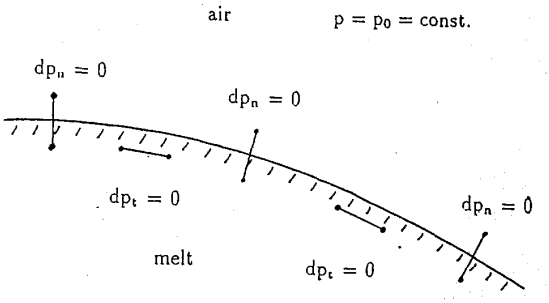

Figure 4: The free surface and the pressure components

$$\nabla \times (\vec{v} \times \vec{\Omega}) = -\frac{\partial(u\,\Omega)}{\partial r} - \frac{\partial(w\,\Omega)}{\partial z} \tag{24}$$

causes a complication in the computation of Navier-Stokes equation. It is the reason for an oscillation in the numerical solution. To avoid this oscillation of the solution the up-wind operator [4,5] has to be applied. Regarding a grid point i,j the up-wind operator for the convection term (24) can be written as follows

$$\frac{\partial(u\,\Omega)}{\partial r} = \frac{u_R\,\Omega_R - u_L\,\Omega_L}{(h_i + h_{i-1})/2} \tag{25}$$

$$\frac{\partial(w\,\Omega)}{\partial z} = \frac{w_T\,\Omega_T - u_B\,\Omega_B}{(k_j + k_{j-1})/2} \tag{26}$$

using the abbreviations

$$u_R = \frac{1}{2}(u_i + u_{i+1}) \quad , \quad u_L = \frac{1}{2}(u_{i-1} + u_i) \tag{27}$$

$$w_T = \frac{1}{2}(w_j + w_{j+1}) \quad , \quad w_B = \frac{1}{2}(w_{j-1} + w_j) \tag{28}$$

$$\Omega_R = \left\{ \begin{array}{ll} \Omega_i & \text{for } u_R \geq 0 \\ \Omega_{i+1} & \text{for } u_R < 0 \end{array} \right\} \tag{29}$$

$$\Omega_L = \left\{ \begin{array}{ll} \Omega_{i-1} & \text{for } u_L \geq 0 \\ \Omega_i & \text{for } u_L < 0 \end{array} \right\} \tag{30}$$

$$\Omega_T = \left\{ \begin{array}{ll} \Omega_j & \text{for } w_T \geq 0 \\ \Omega_{j+1} & \text{for } w_T < 0 \end{array} \right\} \tag{31}$$

$$\Omega_B = \left\{ \begin{array}{ll} \Omega_{j-1} & \text{for } w_B \geq 0 \\ \Omega_j & \text{for } w_B < 0 \end{array} \right\} \tag{32}$$

The special feature of this up-wind operator is the fact that the velocity between two grid points is used. As soon as the vorticity vector $\vec{\Omega}$ is constant the error of discretisation will be of order 2.

VI. COUPLING OF MAGNETIC AND FLUID FLOW FIELD

The electromagnetic forces $\vec{f}_{el}$ in the melt couple the magnetic field and the fluid field. For the study of the fluid flow in the melt the absolute value of $\vec{f}_{el}$ is not significant. The curl of the force determines the intensity of the fluid flow and the form of the vortex. The time average value of the force density is

$$\vec{f}_{el} = \Re\{\vec{\underline{J}} \times \vec{\underline{B}}^*\} \tag{33}$$

The double frequency pulsations do not have an influence because the inertia of the melt is too big in relation to the pulsations [6]. A direct computation of the curl of $\vec{f}_{el}$ is not accurate. It is preferable to obtain it by the field variables [5]. Using the axial symmetric coordinate system one obtains for the φ - component W of the circulation vector $\vec{W}$

$$W = (\vec{W}_\varphi) = (\nabla \times \vec{f}_{el})_\varphi = \Re\{\frac{\partial}{\partial z}(\underline{J}_\varphi \underline{B}_z^*) + \frac{\partial}{\partial r}(\underline{J}_\varphi \underline{B}_r^*)\} \tag{34}$$

Following [7,5] eq. (34) can be transformed to

$$W = (\nabla \times \vec{f}_{el})_\varphi = -\frac{2}{r}\Re\{\underline{J}_\varphi \underline{B}_r^*\} - 2\omega\sigma\Im\{\underline{B}_r \underline{B}_z^*\} \tag{35}$$

Formulation (35) avoids the problems of numerical differentiations.

VII. APPLICATION IN AN INDUSTRIAL CRUCIBLE FURNACE

In dealing with industrial crucible furnaces the knowledge of the induced melting power and the efficiency is of great importance. They can be determined by the analysis of the electromagnetic field. Fig. 2 and 3 show some flux line plots at different load levels and frequencies. A survey of the induced melting power gives the following table. The frequency and the current density are constant.

load level	50 %	75 %	100 %	125 %
induced melting power	504 KW	610 KW	621 KW	612 KW

After the discussion of the solely electromagnetic quantities the computation of the force density $\vec{f}_{el}$ and its curl can be done using the eq. (33) and (35).
Considering the turbulent vortex of the fluid field it is necessary to find the equivalent viscosity η_w. This is done by repeating the computation of the fluid field with different viscosities until condition (21) is satisfied.

In practice the iteration number to find the correct value for the effective viscosity is between 5 to 7.
The computation of the free surface form follows from eq. (23) until condition (22) is satisfied on the surface of the melt. The necessary iterative process is shown in Fig. 6.

It converges quickly, generally after 2 to 3 iterations.

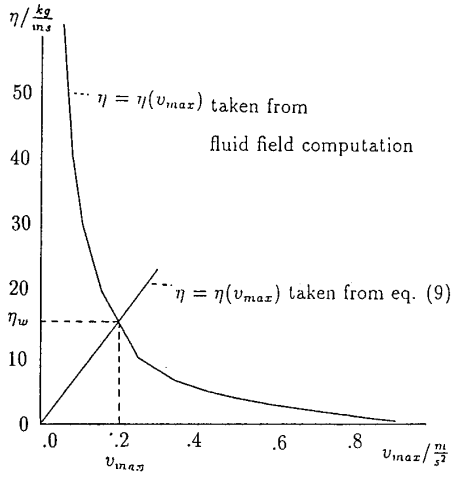

Figure 5: Determination of the effective viscosity η_w

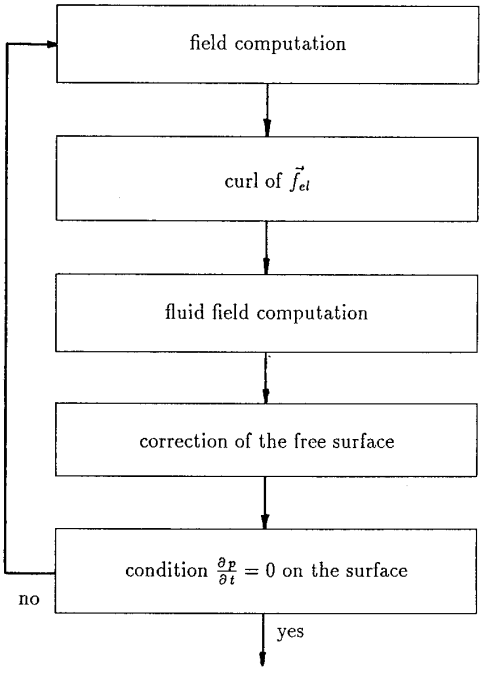

Figure 6: Diagram for the computation of the free surface form

Some computed surface forms including the melting powers are given in Fig. 7. In each case the initial form of the melt is marked by a horizontal line.
The result of a complete solution of the fluid flow problem is given in Fig. 8. Shown are the free surface form and the appropriate fluid field. It is of importance to notice the change of the surface form in relation to the initial condition which is rectangular. The load level of Fig. 8 amounts to 50 % compared with the length of the coil. Of significance is the steep slope of the surface form near the side of the crucible.
An assertion about the fluid velocity in the melt as a function of frequency gives the diagrams in Fig. 9 and 10. The geometry of the inspected crucible furnace can be taken from Fig. 1. The current density is 3.57A/mm^2 in each case. The induced melting

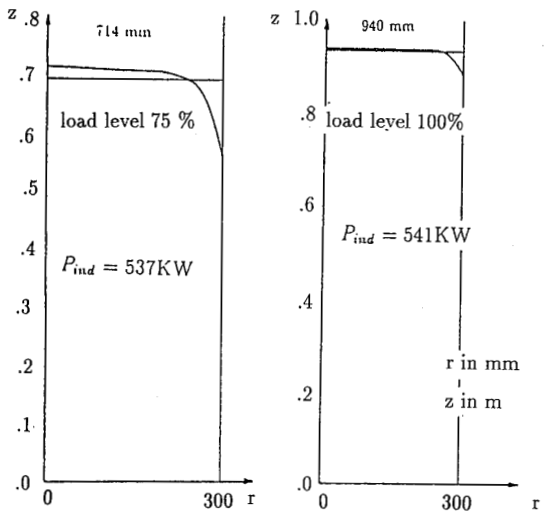

Figure 7: The surface forms of the melt

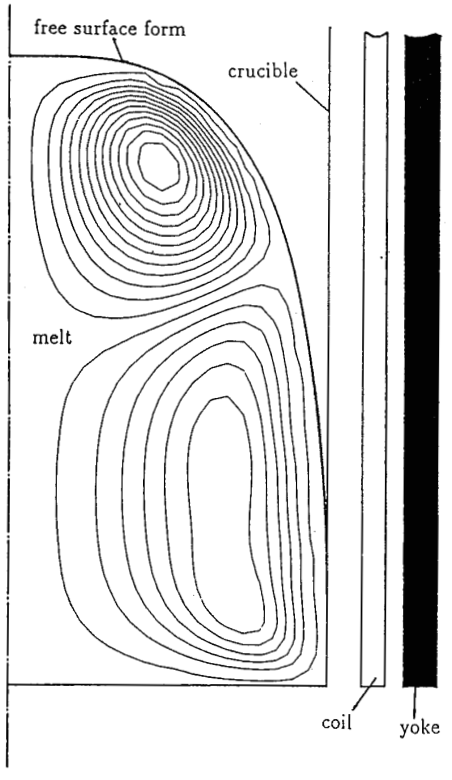

Figure 8: The field of the velocity and the free surface form

power varies according to the frequency. It can be seen in all diagrams that the velocities are lower at lower and higher frequencies and that there is always a maximum of velocity at a particular frequency. The explanation for this trend consists of two parts. At first the induced melting power at lower frequencies is very small. Resulting from these small melting power the vortices of the force in the melt are also small. These small vortices are not able to drive the fluid fast and its velocity becomes low. At high

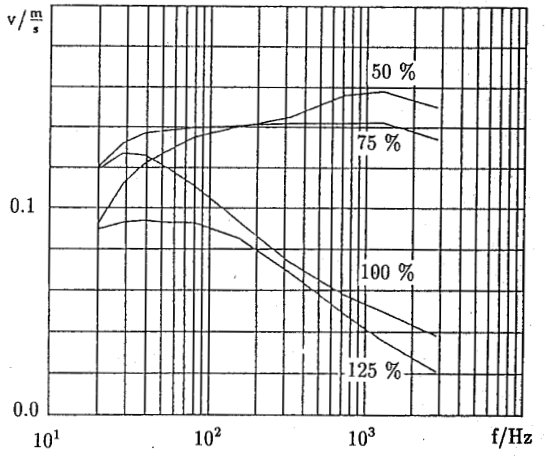

Figure 9: fluid velocity on the surface

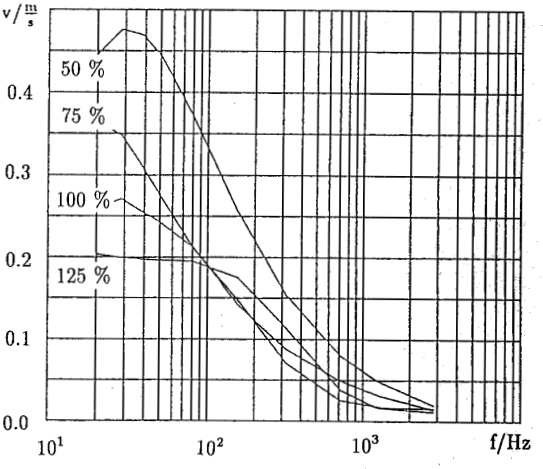

Figure 10: fluid velocity in the axis

frequencies the penetration depth of the magnetic field becomes very small, as does the penetration depth of the electromagnetic force field. The consequence is that the vortices of the fluid field are concentrated near the crucible's side. An even propagation of the vortices including high fluid velocities on the outer surface of the vortices is obviated by this effect. The frequency with the maximum of fluid velocity can be found using this computation method. It is possible to optimize the operation of a crucible furnace. On the one hand an opeartion with high melting power is possible and on the other hand an opeartion with fluid velocities and optimized frequencies can be realized. A comparison with measurements can be taken from [5].

VIII. CONCLUSION

The successful application of the present method has shown that the coupled problem of the magnetic and the fluid flow field can be solved with satisfactorily. The advantages of the finite element method and the finite difference method are fully used and the computation process is stable and clear. With the help of this analysis we can predict and control the intensity of the stirring and the form of the surface and then optimize the coil and the power supply to obtain the optimal intensity of the agitation at the same time the maximum melting power.

References

[1] P.P. Silvester, R.L. Ferrari, *Finite Elements for Electrical Engineers,* Cambridge University Press 1990

[2] W. Albring, *Elementarvorgaenge fluider Wirbelbewegungen,* Akademie-Verlag, Berlin 1981

[3] Ph. Masse, Y. Fautrelle, A. Gagnoud, *Coupled Methods for 3D Coupled Problems 10 Years of Experiments in MHD,* IEEE Transactions on Magnetics, vol.28, no.2, 1275-1278, 1992

[4] P.J. Roache, *Computational fluid dynamics,* hermosa publishers,Albuquerque 1982

[5] L. Leurs, *Untersuchungen ueber die Stroemungsgeschwindigkeit und die Temperaturverteilung in Induktionstiegeloefen,* Doctor Thesis, RWTH Aachen 1988

[6] J.C.R. Hunt, M.R. Maxey, *Estimating velocities and shear stresses in turbulent flows of liquid metals driven by low frequency electromagnetic fields. MHD-Flows and Turbulence,* Israel University Press, Jerusalem 1980

[7] W. Vogt, *Badbewegung und magnetische Feldkraefte beim Induktionstiegelofen.* BBC-Mitteilungen, 56:25-35 1969

[8] E. Taberlet, Y. Fautrelle, *Turbulent stirring in an experimental induction furnace,* Fluid Mechanics, 159:409-431 1985

[9] E.D. Tarapore, J.W. Evans, *Fluid velocities in Induction Melting Furnaces: Part I: Theory and Laboratory Experiments,* Metall. Transactions B, 7B:343-351 1976

[10] E. Truckenbrodt, *Fluid Mechanik,* Springer Verlag, Berlin 1980

[11] J.D. Lavers, M. Ramadan Ahmed, *A Boundary Element Method to predict the Shape of a molten metal free surface in E.M. confinement field,* IEEE Transactions on Magnetics,Vol. 24,No. 6, November 1988

[12] S.R.H. Hoole, *Computer Aided Analysis and Design of Electromagnetic Devices,* Elsevier, New York 1981

Biographical descriptions

G. Henneberger
Mannheim/Germany - born June,16th 1940
married, 2 children
Elementary school in Essen from 1946 to 1950, secondary school in Mannheim from 1950 to 1959, final examination March 1959.
From 1959 to 1965 study of electrical engineering at the TH Karlsruhe, diploma May 1965.
From 1965 to 1966 electrical engineer at BBC in Mannheim, 1966 to 1971 scientific assistant at the Institute of Electrical Machines, University of Technology Aachen.
July,11th. 1970 Dr. PHD, Borchers badge.
From 1971 to 1973 chief engineer at the Institute of Electrical Machines, University of Technology Aachen, at the same time lectureship at the Technical College of Juelich, Germany.
From 1973 to 1988 official in charge (1973), head of a group (1974), head department (1976), head of research (1978) and director of research (1987) at Robert Bosch GmbH, Stuttgart.
From 1986 to 1988 lectureship at the University of Stuttgart.
Since 1988 professor for electrical machines and director of the Institute of Electrical Machines, University of Technology Aachen.
Since 1990 dean of the faculty of electric Engineering of the University of Technology Aachen.

Ph. K. Sattler
Munich/Germany - born September,4th 1923
married
Elementary school in Munich from 1930 to 1934, secondary school in Munich from 1934 to 1942, final examination 1942.
From 1946 to 1949 study at the University of Technology Munich, diploma 1949.
From 1949 to 1954 scientific assistant at the professorship of Electrical Machines and Drives (University of Technology Munich).
From 1954 to 1956 collaborator at Brown Boveri & Cie, Mannheim.
1957 Dr. PHD.
From 1957 to 1964 head of research for all rotating machines produced by BBC, Mannheim, chief engineer (1961), authorized agent (1962).
From 1964 to 1988 professor and director of the Institute of Electrical Machines, University of Technology Aachen.
1983 visiting professor at the University of Tokyo.
Since 1988 retired professor at the Institute of Electrical Machines, University of Technology Aachen.
During the whole time until now many functions at the university and in scientific associations.

Dazhong Shen
Shanghai/China - born February,5th 1960
married, 1 child
Primary school from 1968 to 1973 in Chongqing, China, secondary school from 1973 to 1978 in Chongqing, China.
From 1978 to 1982 study of electrical engineering at the Department of Electrical Engineering, Chongqing University, China.
From 1982 to 1983 postgraduate study by french official aid at Ecole Nationale Superieure d'Ingenieur Electricien de Grenoble (ENSIEG) and Instiut National Polytechnique de Grenoble (INPG), France.
From 1983 to 1987 doctoral postgraduate study.
1987 Dr. PHD.
From 1987 to 1992 scientific assistant at the Institute of Electrical Machines, University of Technology Aachen.
Since 1992 collaborator at SGB, Regensburg Germany.

W. Hadrys
Cologne/Germany - born February,11th 1966
Primary school from 1972 to 1976 in Kerpen, Germany, secondary school from 1976 to 1985 in Bergheim, Germany, final examination 1985.
From 1985 to 1990 study of electrical engineering at the University of Technology Aachen, diploma 1990.
Since 1990 scientific assistant at the Institute of Electrical Machines, University of Technology Aachen.